Bone Research (2013) 1: 85-97.
www.boneresearch.org

ORIGINAL ARTICLE

Osteoblast-restricted Disruption of the Growth Hormone Receptor in Mice Results in Sexually Dimorphic Skeletal Phenotypes

Vandana Singhal[1], Brian C. Goh[1], Mary L. Bouxsein[2], Marie-Claude Faugere[3], Douglas J. DiGirolamo[1]*

[1]Department of Orthopaedic Surgery, Johns Hopkins University School of Medicine, Baltimore, MD, USA; [2]Center for Advanced Orthopedic Studies, Beth Israel Deaconess Medical Center and Harvard Medical School, Boston, MA, USA; [3]Albert B. Chandler Medical Center, University of Kentucky, Lexington, KY, USA

Growth hormone (GH) exerts profound anabolic actions during postnatal skeletal development, in part, through stimulating the production of insulin-like growth factor-1 (IGF-1) in liver and skeletal tissues. To examine the requirement for the GH receptor (GHR) in osteoblast function in bone, we used Cre-LoxP methods to disrupt the GHR from osteoblasts, both *in vitro* and *in vivo*. Disruption of GHR from primary calvarial osteoblasts *in vitro* abolished GH-induced signaling, as assessed by JAK2/STAT5 phosphorylation, and abrogated GH-induced proliferative and anti-apoptotic actions. Osteoblasts lacking GHR exhibited reduced IGF-1-induced Erk and Akt phosphorylation and attenuated IGF-1-induced proliferation and anti-apoptotic action. In addition, differentiation was modestly impaired in osteoblasts lacking GHR, as demonstrated by reduced alkaline phosphatase staining and calcium deposition. In order to determine the requirement for the GHR in bone *in vivo*, we generated mice lacking the GHR specifically in osteoblasts (ΔGHR), which were born at the expected Mendelian frequency, had a normal life span and were of normal size. Three week-old, female ΔGHR mice had significantly reduced osteoblast numbers, consistent with the *in vitro* data. By six weeks of age however, female ΔGHR mice demonstrated a marked increase in osteoblasts, although mineralization was impaired; a phenotype similar to that observed previously in mice lacking IGF-1R specifically in osteoblasts. The most striking phenotype occurred in male mice however, where disruption of the GHR from osteoblasts resulted in a "feminization" of bone geometry in 16 week-old mice, as observed by μCT. These results demonstrate that the GHR is required for normal postnatal bone development in both sexes. GH appears to serve a primary function in modulating local IGF-1 action. However, the changes in bone geometry observed in male ΔGHR mice suggest that, in addition to facilitating IGF-1 action, GH may function to a greater extent than previously appreciated in establishing the sexual dimorphism of the skeleton.

***Keywords*:** growth hormone; osteoblasts; knockout mice; bone; sexual dimorphism

Bone Research (2013) **1**: 85-97. doi: 10.4248/BR201301006

Introduction

Bone acquisition and remodeling depend on the coordinated activities of bone-forming osteoblasts and bone-resorbing osteoclasts. During postnatal development, the activity and lifespan of osteoblasts is regulated by many local growth factors, cytokines, and systemic hormones (1,2). Among these, growth hormone (GH) and insulin-like growth factor-1 (IGF-1) exert anabolic activity, particularly during the rapid phases of bone acquisition that occur during the pubertal growth

*Correspondence: Douglas J. DiGirolamo
E-mail: ddigiro2@jhmi.edu
Tel: 212-870-882
Received 10 January 2013; Accepted 26 January 2013

spurt. GH is a cytokine peptide (3) produced and stored by somatotroph cells of the anterior pituitary. GH functions by binding to its homodimeric transmembrane GH receptor (GHR) and triggering conformational changes (4) that lead to activation of associated JAKs (5-7) to activate STATs (8-16), PI3K/Akt (17, 18) and ERK (19-21). GH-induced activation of STAT5b results in transcriptional activation of IGF-1 (20, 22-24).

In many tissues, GH actions are mediated by its ability to stimulate the production of IGF-1, a widely expressed polypeptide that bears homology to pro-insulin. IGF-1 signals primarily via the heterotetrameric type-1 IGF-1 receptor (IGF-1R) to trigger ERK and PI3K/Akt activation via SHC and insulin receptor substrate-1 and -2 (IRS-1/2) (25,26). IGF-1 is an important growth and survival factor for many cell types, including osteoblasts (27,28). IGF-1 also plays a role in differentiation of fetal rat calvarial osteoblasts to augment type I collagen synthesis and inhibit collagen degradation (29). The role of IGF-1 in bone is well established. For example, osteoblast-specific over-expression of IGF-1 in mice accelerates new bone formation and also increases the rate at which matrix is mineralized (30). Conversely, osteoblast-specific disruption of the IGF-1R results in markedly impaired mineralization of trabecular bone (31).

The precise role of GH in bone has been difficult to define due to the intimate linkage between GH and IGF-1 production. High affinity GH receptors are expressed in osteoblast-like cell lines (32, 33) and in primary mouse osteoblasts (34-36). In addition, GH has been shown to stimulate proliferation of cultured osteoblasts (33). Mice globally deficient in either IGF-1 or GH have impaired postnatal bone acquisition, with the defect being more severe in the IGF-1 nulls (37), suggesting that GH might exert actions independent of IGF-1 in bone. Moreover, treatment of IGF-1 null mice with GH significantly increases mineral apposition and bone formation rates (38). However, interpretation of these models is confounded by the overall growth retardation seen in these mice, as well as problems with reproductive hormone status.

To overcome some of these potentially confounding problems, we used a Cre-LoxP strategy to create a mouse lacking GHR specifically in osteoblasts, which enabled us to determine the requirement of GHR for osteoblast function, both *in vitro* and *in vivo*. Our results demonstrate that the GHR is required for normal postnatal bone development in both sexes. As may be expected, GH appears to serve a primary function in modulating local IGF-1 action. Interestingly, osteoblast-restricted disruption of the GHR in male mice resulted in "feminization" of bone geometry in adult animals, suggesting GH may function to a greater extent than previously appreciated in establishing the sexual dimorphism of the skeleton.

Methods

Materials

Cell culture media, α-minimal essential medium (αMEM), was obtained from Cellgro-Mediatech (Herdon, VA) and fetal bovine serum (FBS) was from Gibco (Gaithersburg, MD). Bovine GH was obtained from the National Hormone and Peptide Program-Monsanto (Torrance, CA) and stored in 200X aliquots for single use. Human IGF-1 was obtained from GroPep (Theberton, SA, Australia) and stored in 1 000X aliquots for single use. Antibodies used for immunoblotting included anti-βactin (C4) from Santa Cruz Biotechnology, Inc. (Santa Cruz, CA); anti-phospho-JAK2 (Tyr1007/1008), anti-JAK2, anti-phospho-STAT5 (Tyr 694), anti-STAT5, anti-phospho-Akt (Ser 473), anti-Akt, anti-phospho-ERK (Thr202/Tyr204), anti-ERK, anti-IGF-1R from Cell Signaling Technology (Danvers, MA), and anti-GHR AL47(a generous gift from Dr. Stuart Frank, University of Alabama at Birmingham, Birmingham, AL). Horseradish-peroxidase conjugated rabbit and mouse secondary antibodies were obtained from Pierce Biotechnology (Rockford, IL). Polyvinylidenedifluoride (PVDF) membrane, Laemmeli sample buffer and other electrophoresis supplies were from Bio-Rad. Assay kits for flow cytometry analysis of cell proliferation were purchased from BD Pharmingen (San Jose, CA). All other reagents not specified here were purchased from Sigma.

Osteoblast isolation and culture

Osteoblasts were isolated from calvaria of newborn $GHR^{fl/fl}$ mice by serial digestion in 1.8 mg·mL^{-1} collagenase type I (Worthington, Lakewood, NJ) solution. Calvaria were digested in 10 mL of digestion solution for 15 min at 37℃ with constant agitation. The digestion solution was collected, and digestion was repeated with fresh digestion solution an additional four times. Digestions 3–5 (containing the osteoblasts) were pooled together, centrifuged, washed with αMEM containing 10% FBS, 1% pen/strep, and plated overnight at 37℃ in a humidified incubator supplied with 5% CO_2. For *in vitro* deletion of the GHR, GHR floxed osteoblasts were cultured to be 70% confluent and then, in the absence of serum, were infected with adenovirus encoding Cre recombinase (Ad-Cre) (Vector Biolabs, Philadelphia, PA) at a titer of 100 multiplicity of infection (moi). Infection with 100 moi of adenovirus encoding green fluorescent protein (Ad-GFP) (Vector Biolabs) was used as control. After 1 hour, culture medium containing 10% FBS was

added and the cells were allowed to recover for the next 48 h. Greater than 90% GHR deletion was confirmed for every infection by quantitative real-time PCR analysis and immunoblotting. For differentiation, osteoblasts were grown to confluence and then switched to differentiation media supplemented with β–glycerophosphate and ascorbic acid for 7 days prior to alkaline phosphatase staining or 14 days prior to alizarin red S staining by standard methods.

Cell lysis and immunoblotting analysis

For signaling experiments, osteoblasts were cultured in αMEM containing 10% FBS, until 90% confluent, and then serum starved in αMEM containing 0.1% FBS for 24 hours to reduce cellular activity to quiescent levels prior to stimulation. At the end of the study, the cells were washed twice with ice-cold phosphate-buffered saline (PBS) and resuspended in lysis buffer (50 mmol·L^{-1} Tris (pH 7.4), 150 mmol·L^{-1} NaCl, 1 mmol·L^{-1} $MgCl_2$, 1 mmol·L^{-1} EDTA, 1% Triton X-100, and 10% glycerol). Protease and phosphatase inhibitors (Sigma) were added to the lysis buffer. The cell lysates were homogenized by needle aspiration and protein concentration was measured by Bradford protein assay (Bio-Rad). For immunoblotting of whole cell lysates, equal amounts of protein (10 or 20 μg per lane) were solubilized in Laemmeli sample buffer and loaded onto a mini-SDS-PAGE system. Following electrophoresis, proteins were transferred to a PVDF membrane using a Bio-Rad semi-dry transfer system. Protein transfer efficiency was verified using pre-stained protein markers. Membranes were then blocked with 5% non-fat dry milk for 1 hour at room temperature and subsequently incubated overnight at 4 ℃ with antibodies directed against the protein of interest. Signals were detected using a horseradish peroxidase-conjugated secondary antibody and bound antibodies were visualized using the Supersignal West Femto Substrate (Pierce). Western blot photographic results were scanned with a Canon flatbed scanner.

Quantitative real-time PCR

Total RNA was extracted from cells using the TRIzol® method, as recommended by the manufacturer (Invitrogen). The RNA concentration was estimated spectrophotometrically and only pure RNA (A260:A280 ratio ≥ 1.8) was used for further analysis. First strand cDNA was synthesized using the iScript cDNA Synthesis Kit (Bio-Rad). The cDNA was amplified in the Opticon Continuous Fluorescent Detector (MJ Research, Waltham, MA) using IQ™ SYBR Green supermix (Bio-Rad) and sequence specific primers. PCR reactions were performed in triplicate for each cDNA, averaged, and normalized to endogenous β-actin reference transcripts. Primer sequences used were as follows: GHR: F5'-GATTTTACCCCCAGTCCCAGTTC-3', R5'-GACCCTTCAGTCTTCTCATCCACA-3'; β-actin: F5'-ACCTCCTACAATGAGCTGC-3', R5'-TGCCAATAGTGATGACCT-3'.

Osteoblast proliferation assays

Osteoblasts were plated in 6-well plates at low cell density (9 x 10^4 cells per well) and cultured in αMEM containing 1% FBS for 24 hours to arrest the cells in G_0 phase. The cells were then stimulated with 500 ng·mL^{-1} GH or 100 ng·mL^{-1} IGF-1 for 48 hours. For proliferation analysis of the cells, 10 μmol·L^{-1} BrdU was added to the medium at the time of mitogenic stimulation. The cells were then stained with anti-BrdU-APC and 7-AAD and analyzed by FACS Calibur (Becton-Dickson). 20 000 events were collected for each sample and results were analyzed with WinMDI version 2.8.

Osteoblast apoptosis assays

Osteoblasts were plated at confluence in 96 well plates in 1% FBS containing media. They were then pretreated for 24 hours with GH or IGF-1 before induction of apoptosis (8 ng·mL^{-1} staurosporine). Apoptosis was assessed by PromegaCaspaseGlo 3/7 according to manufacturer's instructions after 8 hours.

Animal studies

Osteoblast-restricted disruption of the GHR was achieved by crossing mice carrying floxed GHR alleles (GHR$^{fl/fl}$) (39) with mice expressing the Cre recombinase under the control of the human osteocalcin promoter (OC-Cre) (31). Recombination was confirmed in skeletal tissues by allele specific PCR using a forward primer upstream of the floxed exon 4 of GHR, in combination with two reverse primers-one within the floxed exon 4 that resulted in ~720 bp product and one downstream of exon 4 that resulted in ~1 300 bp product following recombination. Male and female control (GHR$^{fl/fl}$) and ΔGHR (GHR$^{fl/fl}$ OC-Cre$^+$) mice were sacrificed at 3, 6, and 16 weeks of age and femurs were removed and fixed in 100% ethanol. Prior to sacrifice, 3- and 6-week-old mice were administered intraperitoneal injections of 100 μL of a 1% calcein solution (to assess dynamic histomorphometric parameters) on a split dose schedule leaving 3 days (for 3-week-old animals) or 5 days (for 6-week-old animals) between the first and second dose, and 2 days (3-week-old) or 3 days (6-week-old) following the second dose before sacrifice. Micro-computed tomography analysis (μCT) of the femur was performed at the Orthopedic Biomechanics Laboratory at Beth Israel Deaconess Medical Center (Boston, MA) and at the

Center for Musculoskeletal Research at Johns Hopkins University. For histomorphometric analysis, femurs were embedded and sectioned. Five serial sections were stained using the Masson-Goldnertrichrome technique, and five more serial sections were left unstained for fluorescent microscopy. Static and dynamic parameters of bone structure and formation were measured at the Albert B. Chandler Medical Center at the University of Kentucky (Lexington, KY).

Statistical analysis

All statistical analyses were performed using the Microsoft Excel data analysis program for ANOVA or Student's t-test analysis with an assigned significance level of 0.05 (α). All experiments were repeated at least three times unless otherwise stated. Values are expressed as a mean±S.E.M.

Results

Disruption of GHR in osteoblasts in vitro abolishes GH signaling and attenuates IGF-1 activity

To examine the requirement of GHR for osteoblast function *in vitro*, primary osteoblasts from mice carrying homozygous floxed GHR alleles were infected with Cre-expressing adenovirus constructs (AdCre) or adenovirus expressing GFP as a control (GFP). Real time PCR analysis of GHR mRNA expression (Figure 1A) showed a 90% reduction in GHR mRNA in osteoblasts infected with 100 moi of AdCre and a complete loss of GHR protein (Figure 1B). Importantly, IGF-1R protein levels were unaffected in AdCre cells (Figure 1B), and infection of wild-type (non-floxed) osteoblasts with AdCre had no discernable effects on basal, GH- or IGF-1-induced ERK or Akt phosphorylation (not shown). GH-induced JAK2, STAT5 and ERK phosphorylation were completely abolished (Figure 1C) following GHR disruption.

Previous studies have described a functional interdependence between GHR and IGF-1R, such that the presence of both receptors is required for each receptor to exert its full competency (40). We therefore examined IGF-1-induced signals in osteoblasts following disruption of GHR. IGF-1-induced ERK activation was blunted in AdCre osteoblasts compared to GFP osteoblasts, and Akt phosphorylation was also reduced (Figure 1C). These results suggest that, in accord with previous observations, GHR is required for full potency of IGF-1R signaling.

Disruption of GHR reduces the proliferative and anti-apoptotic effects of IGF-1

To assess the effect of the GHR on osteoblast proliferation, GFP and AdCre osteoblasts were serum starved for 24 hours and then treated with vehicle, GH or IGF-1. BrdU incorporation, indexed at 48 hours by flow cytometry, showed that both GH and IGF-1 significantly induced BrdU uptake in GFP control cells (Figure 2A). Disruption of GHR abolished GH-induced BrdU uptake and blunted IGF-1-induced BrdU uptake as well (Figure 2A), consistent with the attenuation of IGF-1 signaling observed in the AdCre osteoblasts above (Figure 1C). To determine the requirement of the GHR for osteoblast survival, GFP and AdCre osteoblasts were pre-treated with vehicle, GH or IGF-1 in 1% serum containing media, and then exposed to staurosporine to induce apoptosis. In GFP control osteoblasts, both GH and IGF-1 significantly attenuated staurosporine-induced apoptosis as measured by caspase 3/7 activation (Figure 2B). As expected, disruption of GHR abolished the anti-apoptotic activity of GH (Figure 2B). Moreover, the ability of IGF-1 to attenuate staurosporine-induced apoptosis was also eliminated in ΔGHR osteoblasts (Figure 2B).

Disruption of GHR impairs osteoblast differentiation in vitro

To then assess the effect of GHR signaling on osteoblast differentiation *in vitro*, GFP and AdCre osteoblasts were grown to confluence and before being switched to differentiation media supplemented with β–glycerophosphate and ascorbic acid. AdCre osteoblasts demonstrated a modest, but consistent, reduction in alkaline phosphatase staining at seven days of culture (Figure 2C) and calcium deposition at 14 days of culture (Figure 2D). Taken together, these *in vitro* data suggest that the GHR is required for normal osteoblast function, and further, that loss of the GHR appears to blunt IGF-1R function in osteoblasts.

Osteoblast-restricted disruption of GHR in vivo

To determine the requirement of the GHR for osteoblast function *in vivo*, we conditionally disrupted the GHR in osteoblasts (ΔGHR mice) by crossing GHR floxed mice ($GHR^{fl/fl}$) with mice that express the Cre recombinase under the control of the human osteocalcin promoter (OC-Cre). ΔGHR mice were born at the expected Mendelian frequency, had a normal life span, and exhibited no differences in body weight or length compared to control littermates (not shown). Allele-specific PCR, to identify both the floxed and recombined GHR alleles, demonstrated that recombination occurred only in bone tissues of ΔGHR mice (Figure 3A). μCT measurements were performed at 3, 6 and 16 weeks of age in, both male and female, control and ΔGHR mice. Representative cross-section images of trabecular bone at the distal femur (left) and cortical bone at the femoral

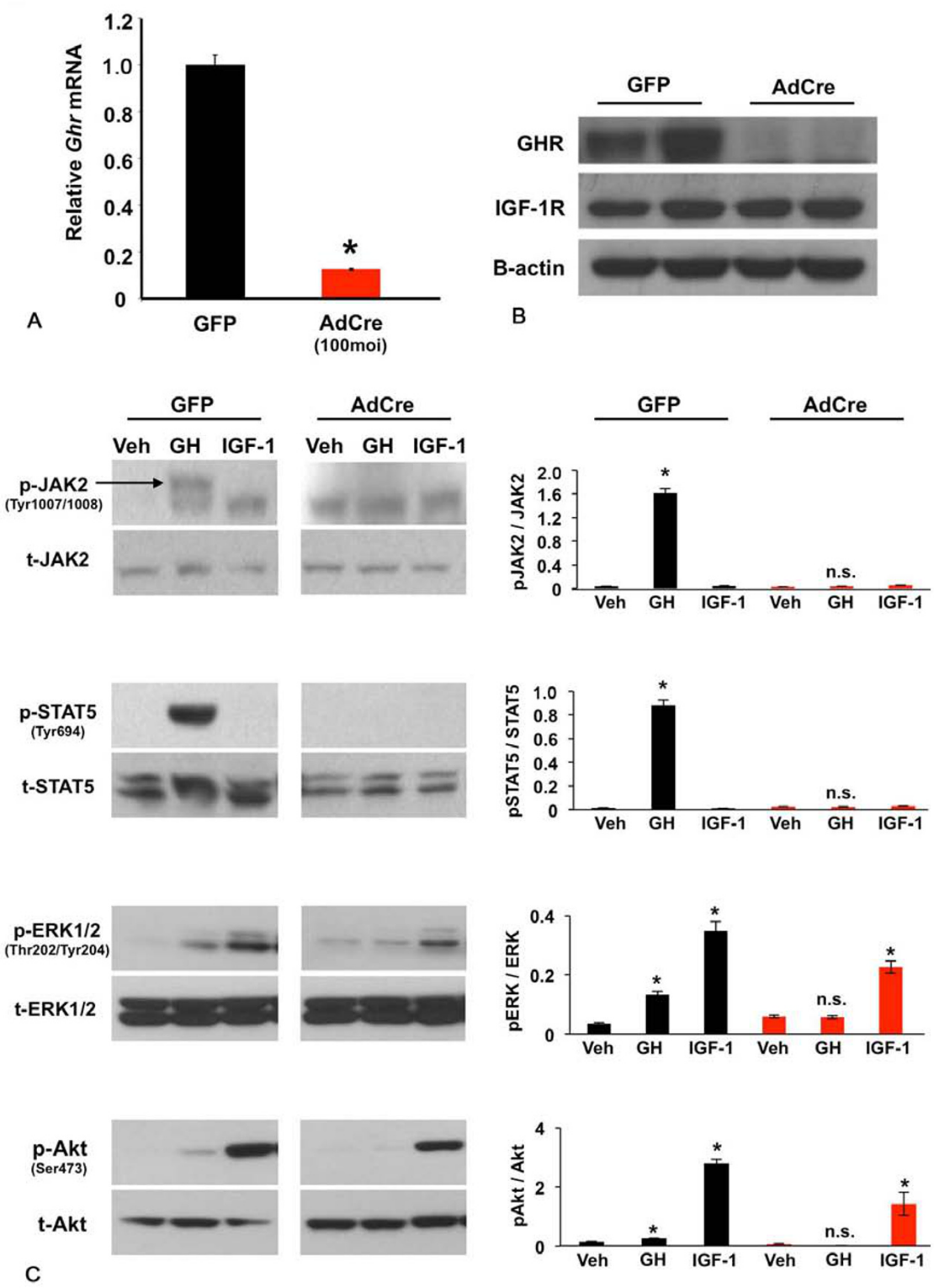

Figure 1 Cre-mediated excision of GHR from primary mouse osteoblasts abolishes GH signaling and attenuates IGF-1 signaling. Calvarial osteoblasts isolated from newborn mice carrying floxed GHR alleles were infected with AdGFP as control or AdCre for deletion. After two days in culture, GHR mRNA expression was assessed by real-time PCR (A), and protein levels of GHR and IGF-1R were analyzed by immunoblotting (B). GFP or AdCre osteoblasts were grown to confluence and serum starved for 24 hours before stimulation with vehicle, GH or IGF-1 for 10 minutes. Cells were lysed and cell lysates immunoblotted with anti-phospho-JAK2 (arrow) and anti-JAK2, anti-phospho-STAT5 and anti-STAT5, anti- phospho-ERK and anti-ERK, or anti-phospho-Akt and anti-Akt (C). Graphs represent densitometric analysis of three experiments. **P*<0.05

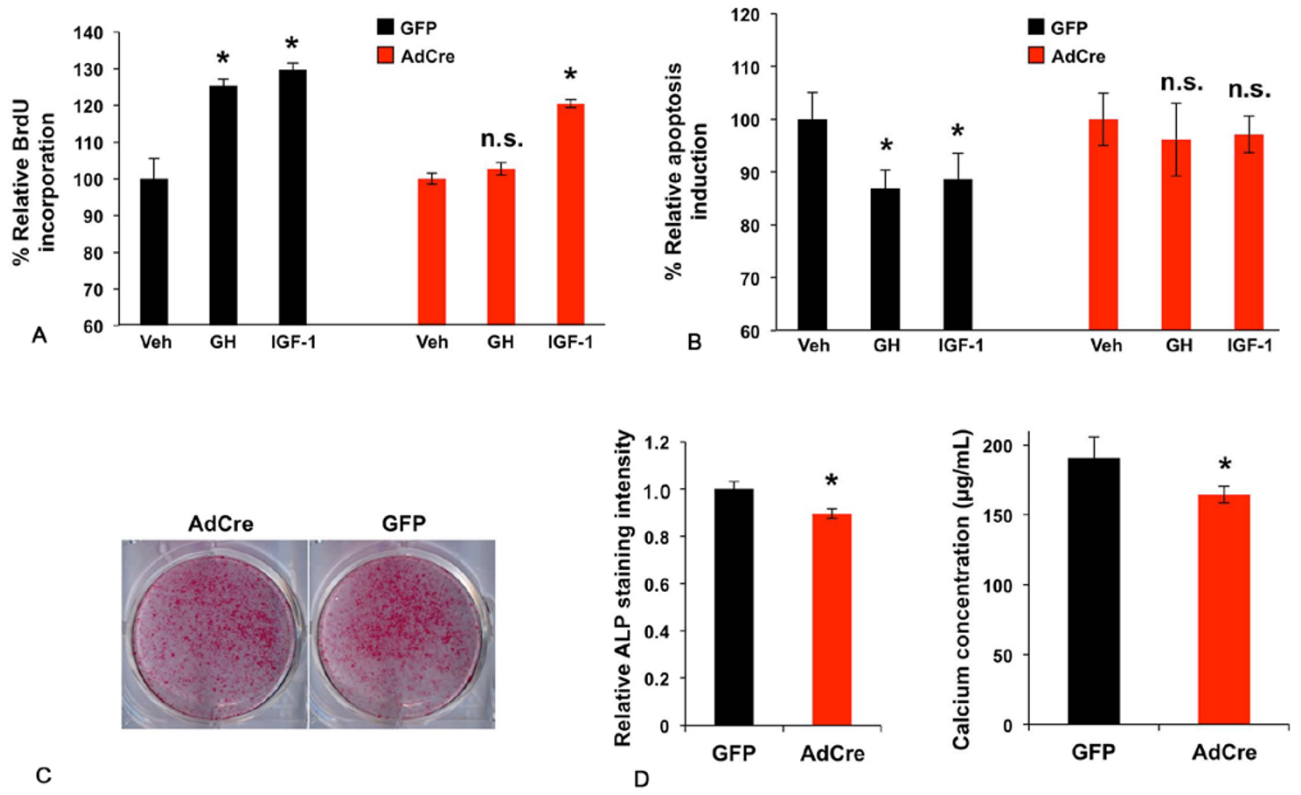

Figure 2 Proliferative and anti-apoptotic actions of IGF-1, as well as osteoblast differentiation, are blunted in osteoblasts lacking GHR. GFP and AdCre osteoblasts were cultured at low density and serum starved for 24 hours before stimulation with GH or IGF-1 to induce proliferation. Proliferation was assessed by BrdU incorporation (A). GFP and AdCre osteoblasts were plated at confluence in 1% FBS containing media and pretreated for 24 hours with GH or IGF-1 before induction of apoptosis (8 ng mL^{-1} staurosporine). Apoptosis was assessed by Promega Caspase- Glo 3/7 after eighthours (B). GFP and AdCre osteoblasts were grown to confluence and then switched to differentiation media for seven days prior to alkaline phosphatase staining (C) or 14 days prior to alizarin red S staining and calcium quantification (D). *P< 0.05

midshaft (right) are shown (Figure 3B-Female, Figure 3C-Male). Complete μCT data for all groups can be found in Table 1. Histomorphometric analysis was performed on the contralateral femur of these same animals, and complete morphometric data are listed in Table 2.

In female ΔGHR mice, μCT analysis revealed only modest changes throughout postnatal development, including a slight increase in cortical thickness and cross-sectional area at three weeks of age and slight cortical thinning at six weeks of age, when compared to controls (Figure 3B and Table 1). However, histomorphometric analysis of trabecular bone in the distal femur revealed a phenotype strikingly similar to that previously observed in female mice with osteoblast-restricted disruption of the IGF-1R (31). At three weeks of age, female ΔGHR mice had less than half the numbers of osteoblasts seen in control mice (Figure 4A). The reduction in osteoblasts in female ΔGHR mice reversed by six weeks of age, such that female ΔGHR mice increased to twice the number of osteoblasts seen in control animals at six weeks (Figure 4B)-again, similar to previous observations in female mice lacking IGF-1R in osteoblasts at six weeks of age. Consistent with the *in vitro* differentiation results, osteoblasts in six-week-old female ΔGHR mice appeared to be functionally impaired, as indicated by reduced bone formation rate per osteoblast and a trend toward increased mineralization lag time (Figure 4C and 4D).

In contrast to female mice, male ΔGHR mice with osteoblast-restricted disruption of the GHR exhibited a skeletal phenotype with age that could be easily appreciated by μCT analysis (Figure 3C and Table 1). While there were no significant changes observed by μCT at earlier ages, 16-week-old male ΔGHR mice had significantly smaller bones than control animals that appeared remarkably similar to bones from female animals, with reduced trabecular bone volume and significantly smaller medullary area (Figure 5A and 5B). Although no differences were observed in osteoblast numbers between control and ΔGHR mice at 16 weeks

Table 1 μCT analysis

Female		Control			ΔGHR		
		3 weeks (*n*=5)	6 weeks (*n*=6)	16 weeks (*n*=5)	3 weeks (*n*=6)	6 weeks (*n*=5)	16 weeks (*n*=7)
Trabecular parameters	BV/TV (%)	13.16 ± 1.07	14.99 ± 1.70	14.80 ± 1.64	15.71 ± 1.35	14.95 ± 1.00	13.33 ± 1.71
	Tb.N (mm^{-1})	4.83 ± 0.24	4.30 ± 0.30	4.33 ± 0.17	5.80 ± 0.40	4.61 ± 0.18	4.19 ± 0.27
	Tb.Th (mm)	38.57 ± 0.52	49.57 ± 0.50	53.60 ± 1.10	39.32 ± 0.70	48.42 ± 0.44	51.96 ± 0.87
	Tb.Sp (mm)	224.33 ± 9.35	239.63 ± 16.85	228.48 ± 10.49	190.38 ±14.91	216.98 ± 8.30	239.94 ±18.09
Cortical parameters	Ct.Th (mm)	89.67 ± 5.24	148.17 ± 4.74	190.80 ± 4.49	101.83 ± 3.15[a]	136.80 ± 2.82[a]	192.14 ± 6.41
	Ct.Ar (mm^2)	0.30 ± 0.03	0.59 ± 0.03	0.71 ± 0.03	0.34 ± 0.02	0.54 ± 0.03	0.72 ± 0.03
	Tt.Ar (mm^2)	1.02 ± 0.07	1.57 ± 0.08	1.50 ± 0.06	1.02 ± 0.07	1.53 ± 0.12	1.49 ± 0.06
	Ma.Ar (mm^2)	0.68 ± 0.05	0.99 ± 0.05	0.77 ± 0.04	0.72 ± 0.05	0.99 ± 0.09	0.79 ± 0.05
	Ct.Ar/Tt.Ar (%)	29.57 ± 1.08	37.37 ± 0.85	47.71 ± 0.94	33.43 ± 0.59[a]	35.47 ± 1.04	48.47 ± 1.63
Male		**Control**			**ΔGHR**		
		3 weeks (*n*=5)	**6 weeks (*n*=5)**	**16 weeks (*n*=5)**	**3 weeks (*n*=5)**	**6 weeks (*n*=8)**	**16 weeks (*n*=5)**
Trabecular parameters	BV/TV (%)	12.88 ± 0.82	22.39 ± 1.28	14.28 ± 1.08	13.95 ± 0.97	23.37 ± 2.01	9.73 ± 0.60[a]
	Tb.N (mm^{-1})	5.21 ± 0.41	6.05 ± 0.22	4.76 ± 0.14	5.00 ± 0.10	6.00 ± 0.25	4.14 ± 0.10[a]
	Tb.Th (mm)	38.92 ± 0.52	50.56 ± 1.96	50.80 ± 0.74	39.10 ± 0.80	52.09 ± 3.33	49.75 ± 1.87
	Tb.Sp (mm)	211.88 ± 19.21	161.16 ± 6.83	207.78 ± 6.43	214.77 ± 4.45	164.48 ± 9.05	238.78 ± 5.78[a]
Cortical parameters	Ct.Th (mm)	98.80 ± 3.07	154.80 ± 4.35	209.00 ± 4.23	97.67 ± 1.86	163.25 ± 3.29	206.43 ± 5.70
	Ct.Ar (mm^2)	0.34 ± 0.02	0.65 ± 0.05	0.88 ± 0.01	0.36 ± 0.03	0.70 ± 0.04	0.83 ± 0.06
	Tt.Ar (mm^2)	1.05 ± 0.06	1.68 ± 0.15	1.92 ± 0.07	1.20 ± 0.13	1.84 ± 0.13	1.68 ± 0.14
	Ma.Ar (mm^2)	0.72 ± 0.04	1.04 ± 0.10	1.07 ± 0.05	0.84 ± 0.10	1.14 ± 0.10	0.88 ± 0.07[a]
	Ct.Ar/Tt.Ar (%)	32.09 ± 0.68	38.64 ± 0.78	46.39 ± 1.34	30.14 ± 0.80	38.74 ± 1.20	49.74 ± 1.04[a]

Trabecular parameters were assessed at the distal femur and cortical parameters at the femoral midshaft. BV/TV–bone volume fraction; Tb.N–trabecular number; Tb.Th–trabecular thickness; Tb.Sp–trabecular separation; Ct.Th–average cortical thickness; Ct.Ar–cortical bone area; Tt.Ar–total cross-sectional area (inside periosteal envelope); Ma.Ar–medullary area; Ct.Ar/Tt.Ar–cortical area fraction. Values shown are mean±SEM.

[a]P<0.05 vs. age-matched control

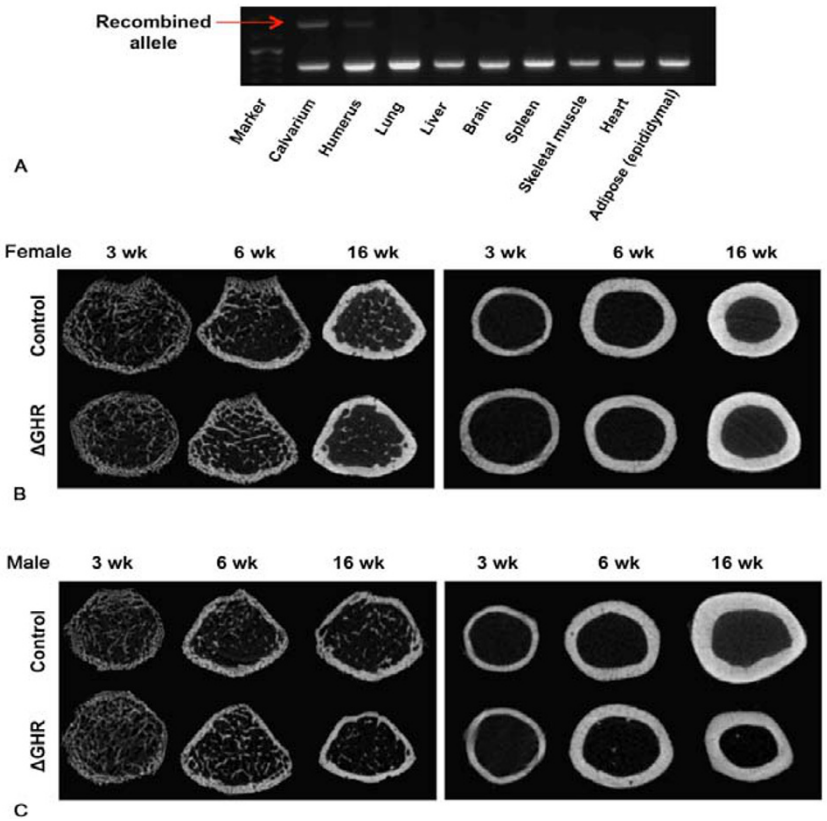

Figure 3 Osteoblast-specific disruption of the GHR *in vivo* results in sexually dimorphic skeletal changes. Allele-specific PCR confirms recombination occurs only in skeletal tissues of ΔGHR mice (A). Representative μCT images of cross sections of trabecular bone in the distal femur (left) and cortical bone in the femoral midshaft (right) from control and ΔGHR mice at the indicated ages are shown for female (B) and male (C) mice.

Table 2 Bone histomorphometry

Female		Control			ΔGHR		
		3 weeks (*n*=5)	6 weeks (*n*=6)	16 weeks (*n*=5)	3 weeks (*n*=6)	6 weeks (*n*=5)	16 weeks (*n*=7)
Bone Structure	BV/TV (%)	5.28 ± 0.79	8.14 ± 1.53	10.86 ± 1.87	7.48 ± 0.64[a]	8.21 ± 0.83	8.06 ± 1.00[a]
	Tb.Th (mm)	16.85 ± 2.01	23.67 ± 1.68	26.29 ± 2.90	19.24 ± 1.34	22.59 ± 1.27	23.55 ± 1.47
	Tb.Sp (mm)	305.20 ± 13.10	272.39 ± 21.14	230.98 ± 26.05	246.02 ± 26.64[a]	275.09 ± 39.11	303.93 ± 55.05
Bone Formation	OV/BV (%)	5.08 ± 1.31	1.98 ± 0.35	4.73 ± 0.47	2.91 ± 0.49[a]	6.19 ± 1.58[a]	4.34 ± 1.42
	OS/BS (%)	21.42 ± 5.00	12.53 ± 2.24	21.25 ± 1.40	13.82 ± 2.10[a]	26.83 ± 4.68[a]	19.32 ± 3.26
	O.Th (mm)	1.95 ± 0.19	1.93 ± 0.23	2.88 ± 0.27	1.99 ± 0.23	2.52 ± 0.42	2.29 ± 0.23
	Ob.S/BS (%)	23.81 ± 6.95	10.25 ± 2.47	7.57 ± 1.72	7.04 ± 2.67[a]	20.73 ± 2.22[a]	10.07 ± 3.67
	N.Ob/B.Pm (no./100mm)	3256.37 ± 1074.69	1065.70 ± 234.94	822.50 ± 159.03	1063.82 ± 360.88[a]	2433.80 ± 302.03[a]	1093.11 ± 392.20
Bone Erosion	ES/BS (%)	6.25 ± 1.15	9.55 ± 0.84	8.51 ± 2.19	7.04 ± 1.24	6.49 ± 2.38[a]	6.85 ± 1.06
	E.De (mm)	5.96 ± 1.23	4.84 ± 0.28	6.81 ± 0.26	6.03 ± 0.27	6.16 ± 0.41[a]	6.96 ± 0.33
	Oc.S/BS (%)	6.01 ± 1.20	7.95 ± 0.80	7.62 ± 2.03	9.35 ± 3.24	5.25 ± 1.96[a]	5.86 ± 0.94
	N.Oc/B.Pm (no./100mm)	333.58 ± 100.17	379.94 ± 31.49	373.06 ± 98.63	455.53 ± 136.94	306.34 ± 98.73	318.96 ± 44.21
Bone Dynamics	MAR (day)	0.90 ± 0.16	1.60 ± 0.24		0.83 ± 0.12	1.31 ± 0.08	
	MS/BS (%)	12.48 ± 1.52	15.11 ± 2.21		13.95 ± 2.26	21.34 ± 3.58[a]	
	BFR/BS ($\mu m^3/\mu m^2/d$)	3.96 ± 0.58	8.27 ± 1.23		4.50 ± 1.42	10.28 ± 2.07	
	BFR/N.Ob (mm^2/Ob/y)	2.02 ± 1.23	9.62 ± 2.22		12.47 ± 6.12[a]	4.35 ± 0.87[a]	
	Mlt (day)	5.11 ± 1.64	1.67 ± 0.66		3.39 ± 0.73	3.09 ± 0.81	

Male		Control			ΔGHR		
		3 weeks (*n*=5)	6 weeks (*n*=5)	16 weeks (*n*=5)	3 weeks (*n*=5)	6 weeks (*n*=8)	16 weeks (*n*=5)
Bone Structure	BV/TV (%)	7.93 ± 1.75	7.00 ± 1.04	7.97 ± 2.94	7.33 ± 1.64	10.97 ± 1.59[a]	6.71 ± 1.01
	Tb.Th (mm)	17.16 ± 1.69	23.12 ± 1.15	24.57 ± 2.40	15.90 ± 3.01	26.77 ± 1.99	21.17 ± 1.08
	Tb.Sp (mm)	224.15 ± 38.92	333.33 ± 51.57	448.96 ± 137.20	204.27 ± 15.89	242.38 ± 30.04[a]	306.35 ± 28.09
Bone Formation	OV/BV (%)	4.13 ± 1.01	1.34 ± 0.60	5.16 ± 1.33	4.65 ± 2.12	2.15 ± 0.59	5.77 ± 2.64
	OS/BS (%)	17.35 ± 3.81	6.70 ± 2.16	22.02 ± 6.22	13.53 ± 2.42	10.98 ± 2.52	23.36 ± 6.22
	O.Th (mm)	1.95 ± 0.13	2.05 ± 0.27	2.94 ± 0.24	2.26 ± 0.18	2.47 ± 0.33	2.29 ± 0.36
	Ob.S/BS (%)	9.20 ± 3.00	7.18 ± 4.85	2.80 ± 1.30	11.77 ± 0.52	10.39 ± 2.02	2.00 ± 0.58
	N.Ob/B.Pm (no./100mm)	1216.61 ± 248.42	567.28 ± 325.23	263.12 ± 106.59	1735.86 ± 119.14[a]	1016.92 ± 207.13	228.74 ± 68.71
Bone Erosion	ES/BS (%)	7.10 ± 1.26	3.61 ± 0.79	6.88 ± 1.02	8.26 ± 0.52	3.30 ± 0.78	3.94 ± 1.02[a]
	E.De (mm)	6.65 ± 0.93	6.16 ± 0.30	6.59 ± 0.65	5.07 ± 0.23	6.87 ± 0.74	5.05 ± 0.35[a]
	Oc.S/BS (%)	6.25 ± 1.17	3.03 ± 0.59	5.58 ± 0.57	6.96 ± 0.52	2.92 ± 0.74	3.63 ± 0.97[a]
	N.Oc/B.Pm (no./100mm)	338.43 ± 72.74	165.52 ± 21.63	289.08 ± 26.85	446.65 ± 59.48	137.87 ± 35.86	157.53 ± 25.60[a]
Bone Dynamics	MAR (day)	1.13 ± 0.14	2.05 ± 0.18		0.89 ± 0.19	1.86 ± 0.17	
	MS/BS (%)	12.16 ± 3.22	20.54 ± 4.77		11.71 ± 1.67	17.33 ± 2.43	
	BFR/BS ($\mu m^3/\mu m^2/d$)	5.54 ± 2.25	15.41 ± 4.18		3.99 ± 1.20	12.49 ± 2.71	
	BFR/N.Ob (mm^2/Ob/y)	5.15 ± 2.21	64.61 ± 31.04		2.25 ± 0.62	14.81 ± 2.52[a]	
	Mlt (day)	3.24 ± 0.48	0.38 ± 0.08		4.39 ± 1.66	1.14 ± 0.32[a]	

Histomorphometry was performed in trabecular bone of the distal femur. BV/TV–Bone volume/tissue volume; Tb.Th–Trabecular thickness; Tb.Sp–Trabecular separation; OV/BV–Osteoid volume/bone volume; OS/BS–Osteoid surface/bone surface; O.Th–Osteoid thickness; Ob.S/BS–Osteoblast surface/bone surface; N.Ob/B.Pm–Osteoblast number/bone perimeter; ES/BS–Erosion surface/bone surface; E.De–Erosion depth; Oc.S/BS–Osteoblast surface; N.Oc/B.Pm–Osteoclast number/bone perimeter; MAR–Mineral apposition rate; MS/BS–Mineralizing surface/bone surface; BFR/BS–Bone formation rate/bone surface; BFR/N.Ob–Bone formation rate/osteoblast; Mlt–Mineralization lag time. Values shown are mean±S.E.M.

[a]$P<0.05$ vs. age-matched control

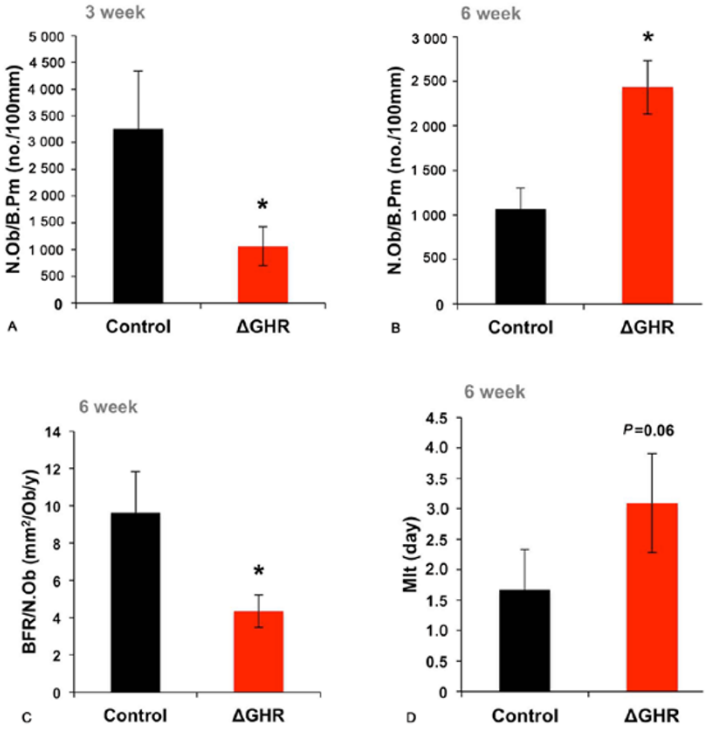

Figure 4 Selected histomorphometric parameters from 3-week (A) and 6-week (B, C and D) female mice. **P*<0.05

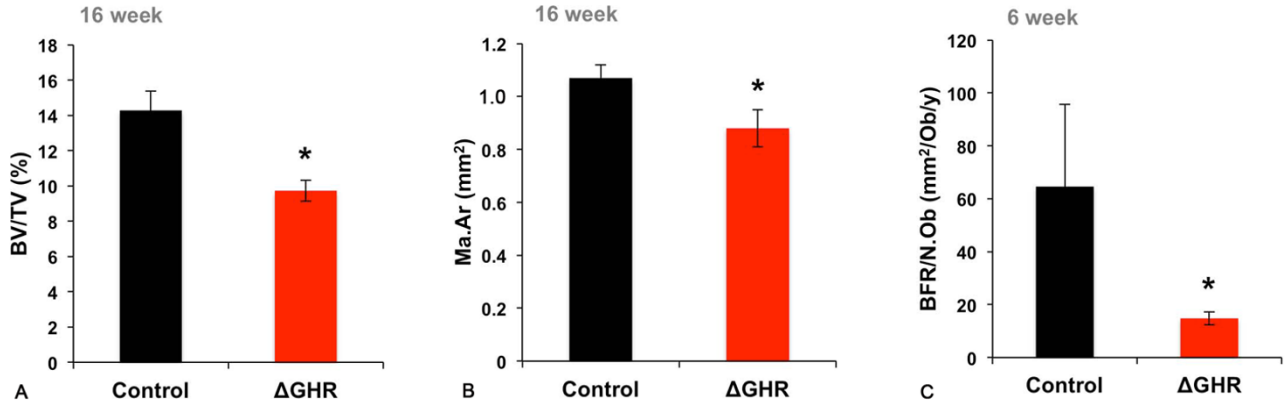

Figure 5 Select μCT (A and B) and histomorphometric parameters (C) from male mice. **P*<0.05

of age, osteoblasts in male ΔGHR mice at six weeks of age appeared to perform more poorly than in control animals, as indicated by a significantly reduced bone formation rate per osteoblast (Figure 5C). Unfortunately, this dynamic histomorphometric measurement cannot be performed in 16-week-old mice to directly assess osteoblast activity at this age. Together, these *in vivo* data suggest that, although much of GH action in promoting skeletal development would appear to result from stimulating IGF-1 production, the GHR plays a distinct role in establishing the sexual dimorphism observed in the skeleton of adult mice.

Discussion

In this study, we used a genetic approach to disrupt the GHR in an osteoblast-restricted manner, enabling us to distinguish the contribution of GHR mediated signals to osteoblast function. The loss of GHR in osteoblasts *in vitro* diminished both the proliferative and anti-apoptotic effects of IGF-1 and impaired modestly osteoblast differentiation. Interestingly, osteoblasts lacking GHR had normal levels of IGF-1R protein but demonstrated reduced IGF-1-induced ERK and Akt phosphorylation. This result suggests that the presence of the GHR protein

itself is required for full signaling efficacy of the IGF-1R, in agreement with previous studies that have described synergistic interactions between the GHR and IGF-1R. For example, in GHR expressing melanocytes, GH administration alone had no effect on proliferation, whereas IGF-1 significantly increased cell numbers, and the combination of both growth factors amplified this response by 50% (41). In addition, GH pre-treatment of cultured human osteoblasts increased osteoblast sensitivity to subsequent IGF-1 treatment (42). Moreover, previous work from our group (40) showed that GH-induced STAT5 phosphorylation is attenuated in mouse osteoblasts that lack the IGF-1R. Together, these observations suggest the presence of a mechanism whereby the response of these cell types to GH and IGF-1 is maximal only when both receptors are present. One possible mechanism is suggested by studies of Huang *et al* (43), who demonstrated that increased GH signaling potency in pre-adipocytes involves a physical interaction between GHR, JAK2 and IGF-1R. In their studies, JAK2 physically associated with GHR and IGF-1R, and this complex then bound and phosphorylated SHC to activate downstream signaling pathways (44). In this scenario, loss of GHR and the associated JAK2 kinase may cause impaired IGF-1-induced recruitment and/or phosphorylation of SHC-Grb2-SOS. Such a mechanism would be compatible with the reduced IGF-1-induced ERK and Aktphosphorylation seen in our ΔGHR osteoblasts. Additional studies, to more definitively characterize the molecular mechanisms that mediate GHR/IGF-1R interactions, are ongoing in our laboratory.

The changes observed in skeletal phenotype following loss of the GHR *in vivo* suggest both distinct and overlapping roles for GH and IGF-1 in postnatal bone acquisition. The histomorphometric changes observed in trabecular bone in female ΔGHR mice closely resembled those described previously in female mice lacking the IGF-1R in osteoblasts (31). For example, both female ΔGHR and ΔIGF-1R mutants demonstrated reduced trabecular osteoblast numbers at three weeks of age. These findings are compatible with the current *in vitro* observations of abolished GH-induced, and subsequent blunting of IGF-1-induced, proliferative/anti-apoptotic actions, demonstrating the importance of GH/IGF-1 in regulating osteoblast numbers in early development. Unlike female mice lacking IGF-1R in osteoblasts however, three-week-old female ΔGHR mice did not have lower bone volume compared to control animals. By contrast, female ΔGHR mice actually had increased trabecular bone volume at this age despite the reduction in osteoblast numbers, likely resulting from a dramatic increase in bone formation rate per osteoblast (12.47±6.12 *vs.* 2.02±1.23 mm^2/Ob/yin controls). The increase in trabecular bone volume, despite reduced osteoblast numbers at three weeks of age in female ΔGHR mice, suggests that up-regulation of local IGF-1 via mechanisms other than GH might be able to compensate for the lack of GH-induced IGF-1 production from osteoblasts in control animals. In support of this notion, three-week-old, female transgenic mice in which IGF-1 was over-expressed specifically in osteoblasts had increased trabecular bone volume and dramatically increased measures of bone formation, with no change in the number of osteoblasts (30). By six weeks of age, female ΔGHR mice had nearly twice the number of osteoblasts compared to control animals and increased mineralization lag time; a histological picture, again, analogous to that previously observed in ΔIGF-1R mice (31). It appears likely that the increased numbers of osteoblasts in both mutants represent compensation by other growth factors in response to loss of GH/IGF-1 action. The inability to maintain normal bone volume later in life, despite the increase in osteoblast numbers, may relate to the reduced differentiation capacity observed in osteoblasts lacking the GHR *in vitro*. In addition, this deficiency in bone volume could owe to other components of the GH/IGF-1 system, namely, IGF binding proteins (IGFBP). For example, IGFBP5 levels increased dramatically at three weeks of age in the IGF-1 over-expressing mice mentioned above, coincident with the increase in osteoblast function (45). However, IGFBP5 levels decreased by six weeks of age, in both wild type and transgenic mice, when osteoblast activity had returned to normal in the IGF-1 over-expressing mice; presenting the possibility that reduced matrix-bound IGFBP5 might diminish the capacity of IGF-1 to stimulate bone formation in older animals (45), since matrix-bound IGFBP5 has been shown to potentiate IGF signaling (46, 47).

The alterations described above in female ΔGHR mice suggest significant overlap in GH and IGF-1 function in osteoblasts. Namely, GH appears to stimulate local IGF-1 production, and the GHRfacilitates maximal IGF-1 action. However, the dramatic skeletal phenotype observed in 16-week-old male ΔGHR mice-an apparent "feminization" of the femur (not observed in ΔIGF-1R mice)-indicates a significant difference in the interaction of GH and IGF-1 with sex steroids. Indeed, mice exhibit profound sex-dependent differences in the pulsatility and amplitude of GH secretion that results in sexually dimorphic expression of GH target genes (48), providing one possible explanation for the gender specificity of the phenotypes the ΔGHR mice. Alternatively, it is known that osteoblasts that reside at the periosteal surface

arise from precursors distinct from osteoblasts in the trabecular compartment, and evidence suggests these cells may have a differential response to PTH and estrogen (49). In addition, numerous studies, in both humans and animal models, have demonstrated that estrogen is predominantly responsible for periosteal expansion in males, converted from androgens by aromatase (50). In this regard, aromatase expression in bone is regulated by a promoter responsive to class I cytokines (51), and the GHR is class I cytokine receptor (52). Thus, it is an intriguing possibility, currently under investigation, that the failure of periosteal expansion observed in male ΔGHR mice might result from a reduction of GH-stimulated aromatase expression, and thus, ironically, the resultant lack of converted estrogen that would normally stimulate periosteal expansion produces a more "feminine" bone in male ΔGHR mice, while estrogen-replete females remain unaffected.

In summary, our studies demonstrate that the GHR is required for normal postnatal bone development in both sexes. As may be expected, GH appears to serve a primary function in modulating local IGF-1 action. However, osteoblast-restricted disruption of the GHR in male mice resulted in "feminization" of bone geometry in adult animals, suggesting GH may function to a greater extent than previously appreciated in establishing the sexual dimorphism of the skeleton.

Acknowledgements

The authors thank Drs. Yong Fan and Mark Sperling for providing the $GHR^{fl/fl}$ mice. This work was supported by grants from the NIH: R01 AR052746 to TLC and R01 AR062074 to DJD.

References

1 Karsenty G. Bone formation and factors affecting this process. Matrix Biol. 2000 ;19:85-89.

2 Mundy GR, Boyce B, Hughes D, Wright K, Bonewald L, Dallas S, Harris S, Ghosh-Choudhury N, Chen D, Dunstan C. The effects of cytokines and growth factors on osteoblastic cells. Bone. 1995;17:71S-75S.

3 Miller WL, Eberhardt NL. Structure and evolution of the growth hormone gene family. Endocr Rev. 1983;4:97-130.

4 Yang N, Langenheim JF, Wang X, Jiang J, Chen WY, Frank SJ. Activation of growth hormone receptors by growth hormone and growth hormone antagonist dimers: insights into receptor triggering. Mol Endocrinol. 2008;22:978-988.

5 Argetsinger LS, Campbell GS, Yang X, Witthuhn BA, Silvennoinen O, Ihle JN, Carter-Su C. Identification of JAK2 as a growth hormone receptor-associated tyrosine kinase. Cell. 1993;74:237-244.

6 Foster CM, Shafer JA, Rozsa FW, Wang XY, Lewis SD, Renken DA, Natale JE, Schwartz J, Carter-Su C. Growth hormone promoted tyrosyl phosphorylation of growth hormone receptors in murine 3T3-F442A fibroblasts and adipocytes. Biochemistry. 1988;27:326-334.

7 Silva CM, Day RN, Weber MJ, Thorner MO. Human growth hormone (GH) receptor is characterized as the 134-kilodalton tyrosine-phosphorylated protein activated by GH treatment in IM-9 cells. Endocrinology. 1993;133:2307-2312.

8 Bergad PL, Shih HM, Towle HC, Schwarzenberg SJ, Berry SA. Growth hormone induction of hepatic serine protease inhibitor 2.1 transcription is mediated by a Stat5-related factor binding synergistically to two gamma-activated sites. J Biol Chem. 1995; 270:24903-24910.

9 Campbell GS, Meyer DJ, Raz R, Levy DE, Schwartz J, Carter-Su C. Activation of acute phase response factor (APRF)/Stat3 transcription factor by growth hormone. J Biol Chem. 1995;270: 3974-3979.

10 Choi HK, Waxman DJ. Pulsatility of growth hormone (GH) signalling in liver cells: role of the JAK-STAT5b pathway in GH action. Growth Horm IGF Res. 2000;10 Suppl B:S1-S8.

11 Delesque-Touchard N, Park SH, Waxman DJ. Synergistic action of hepatocyte nuclear factors 3 and 6 on CYP2C12 gene expression and suppression by growth hormone-activated STAT5b. Proposed model for female specific expression of CYP2C12 in adult rat liver. J Biol Chem. 2000;275:34173-34182.

12 Lahuna O, Rastegar M, Maiter D, Thissen JP, Lemaigre FP, Rousseau GG. Involvement of STAT5 (signal transducer and activator of transcription 5) and HNF-4 (hepatocyte nuclear factor 4) in the transcriptional control of the hnf6 gene by growth hormone. Mol Endocrinol. 2000;14:285-294.

13 Meyer DJ, Campbell GS, Cochran BH, Argetsinger LS, Larner AC, Finbloom DS, Carter-Su C, Schwartz J. Growth hormone induces a DNA binding factor related to the interferon-stimulated 91-kDa transcription factor. J Biol Chem. 1994;269:4701-4704.

14 Sotiropoulos A, Moutoussamy S, Binart N, Kelly PA, Finidori J. The membrane proximal region of the cytoplasmic domain of the growth hormone receptor is involved in the activation of Stat 3. FEBS Lett. 1995;369:169-172.

15 Waxman DJ. Growth hormone pulse-activated STAT5 signalling: a unique regulatory mechanism governing sexual dimorphism of liver gene expression. Novartis Found Symp. 2000;227:61-74.

16 Waxman DJ, Ram PA, Park SH, Choi HK. Intermittent plasma growth hormone triggers tyrosine phosphorylation and nuclear translocation of a liver-expressed, Stat 5-related DNA binding protein. Proposed role as an intracellular regulator of male-specific liver gene transcription. J Biol Chem. 1995;270:13262-13270.

17 Costoya JA, Finidori J, Moutoussamy S, Searis R, Devesa J, Arce VM. Activation of growth hormone receptor delivers an antiapoptotic signal: evidence for a role of Akt in this pathway. Endocrinology. 1999;140:5937-5943.
18 Liang L, Jiang J, Frank SJ. Insulin receptor substrate-1-mediated enhancement of growth hormone-induced mitogen-activated protein kinase activation. Endocrinology. 2000;141:3328-3336.
19 Campbell GS, Pang L, Miyasaka T, Saltiel AR, Carter-Su C. Stimulation by growth hormone of MAP kinase activity in 3T3-F442A fibroblasts. J Biol Chem. 1992;267:6074-6080.
20 Moller C, Hansson A, Enberg B, Lobie PE, Norstedt G. Growth hormone (GH) induction of tyrosine phosphorylation and activation of mitogen-activated protein kinases in cells transfected with rat GH receptor cDNA. J Biol Chem. 1992;267:23403-23408.
21 Winston LA, Bertics PJ. Growth hormone stimulates the tyrosine phosphorylation of 42- and 45-kDa ERK-related proteins. J Biol Chem. 1992;267:4747-4751.
22 Frank SJ, Yi W, Zhao Y, Goldsmith JF, Gilliland G, Jiang J, Sakai I, Kraft AS. Regions of the JAK2 tyrosine kinase required for coupling to the growth hormone receptor. J Biol Chem. 1995;270: 14776-14785.
23 Sotiropoulos A, Perrot-Applanat M, Dinerstein H, Pallier A, Postel-Vinay MC, Finidori J, Kelly PA. Distinct cytoplasmic regions of the growth hormone receptor are required for activation of JAK2, mitogen-activated protein kinase, and transcription. Endocrinology. 1994;135:1292-1298.
24 VanderKuur JA, Wang X, Zhang L, Campbell GS, Allevato G, Billestrup N, Norstedt G, Carter-Su C. Domains of the growth hormone receptor required for association and activation of JAK2 tyrosine kinase. J Biol Chem. 1994;269:21709-21717.
25 Dietrich P, Dragatsis I, Xuan S, Zeitlin S, Efstratiadis A. Conditional mutagenesis in mice with heat shock promoter-driven cre transgenes. Mamm Genome. 2000;11:196-205.
26 LeRoith D. Insulin-like growth factor I receptor signaling-overlapping or redundant pathways? Endocrinology. 2000;141: 1287-1288.
27 Hill PA, Tumber A, Meikle MC. Multiple extracellular signals promote osteoblast survival and apoptosis. Endocrinology. 1997;138:3849-3858.
28 Merriman HL, La Tour D, Linkhart TA, Mohan S, Baylink DJ, Strong DD. Insulin-like growth factor-I and insulin-like growth factor-II induce c-fos in mouse osteoblastic cells. Calcif Tissue Int. 990;46:258-262.
29 Rydziel S, Delany AM, Canalis E. Insulin-like growth factor I inhibits the transcription of collagenase 3 in osteoblast cultures. J Cell Biochem. 1997;67:176-183.
30 Zhao G, Monier-Faugere MC, Langub MC, Geng Z, Nakayama T, Pike JW, Chernausek SD, Rosen CJ, Donahue LR, Malluche HH, Fagin JA, Clemens TL. Targeted overexpression of insulin-like growth factor I to osteoblasts of transgenic mice: increased trabecular bone volume without increased osteoblast proliferation. Endocrinology. 2000;141:2674-2682.
31 Zhang M, Xuan S, Bouxsein ML, von Stechow D, Akeno N, Faugere MC, Malluche H, Zhao G, Rosen CJ, Efstratiadis A, Clemens TL. Osteoblast-specific knockout of the insulin-like growth factor (IGF) receptor gene reveals an essential role of IGF signaling in bone matrix mineralization. J Biol Chem. 2002; 277:44005-44012.
32 Barnard R, Ng KW, Martin TJ, Waters MJ. Growth hormone (GH) receptors in clonal osteoblast-like cells mediate a mitogenic response to GH. Endocrinology. 1991;128:1459-1464.
33 Nilsson A, Swolin D, Enerback S, Ohlsson C. Expression of functional growth hormone receptors in cultured human osteoblast-like cells. J Clin Endocrinol Metab. 1995;80:3483-3488.
34 Scheven BA, Hamilton NJ, Fakkeldij TM, Duursma SA. Effects of recombinant human insulin-like growth factor I and II (IGF-I/-II) and growth hormone (GH) on the growth of normal adult human osteoblast-like cells and human osteogenic sarcoma cells. Growth Regul. 1991;1:160-167.
35 Slootweg MC, Salles JP, Ohlsson C, de Vries CP, Engelbregt MJ, Netelenbos JC. Growth hormone binds to a single high affinity receptor site on mouse osteoblasts: modulation by retinoic acid and cell differentiation. J Endocrinol. 1996;150:465-472.
36 Slootweg MC, van Buul-Offers SC, Herrmann-Erlee MP, van der Meer JM, Duursma SA. Growth hormone is mitogenic for fetal mouse osteoblasts but not for undifferentiated bone cells. J Endocrinol. 1988;116:11-13.
37 Mohan S, Richman C, Guo R, Amaar Y, Donahue LR, Wergedal J, Baylink DJ. Insulin-like growth factor regulates peak bone mineral density in mice by both growth hormone-dependent and -independent mechanisms. Endocrinology. 2003;144:929-936.
38 Bikle D, Majumdar S, Laib A, Powell-Braxton L, Rosen C, Beamer W, Nauman E, Leary C, Halloran B. The skeletal structure of insulin-like growth factor I-deficient mice. J Bone Miner Res. 2001;16:2320-2329.
39 Fan Y, Menon RK, Cohen P, Hwang D, Clemens T, DiGirolamo DJ, Kopchick JJ, Le Roith D, Trucco M, Sperling MA. Liver-specific deletion of the growth hormone receptor reveals essential role of growth hormone signaling in hepatic lipid metabolism. J Biol Chem. 2009;284:19937-19944.
40 DiGirolamo DJ, Mukherjee A, Fulzele K, Gan Y, Cao X, Frank SJ, Clemens TL. Mode of growth hormone action in osteoblasts. J Biol Chem. 2007;282:31666-31674.
41 Edmondson SR, Russo VC, McFarlane AC, Wraight CJ, Werther GA. Interactions between growth hormone, insulin-like growth factor I, and basic fibroblast growth factor in melanocyte growth. J Clin Endocrinol Metab. 1999;84:1638-1644.
42 Langdahl BL, Kassem M, Moller MK, Eriksen EF. The effects of IGF-I and IGF-II on proliferation and differentiation of human osteoblasts and interactions with growth hormone. Eur J Clin

Invest. 1998;28:176-183.

43 Huang Y, Kim S-O, Yang N, Jiang J, Frank SJ. Physical and functional interaction of growth hormone and insulin-like growth factor-I signaling elements. Mol Endocrinol. 2004;18:1471-1485.

44 Le Roith D, Bondy C, Yakar S, Liu JL, Butler A. The somatomedin hypothesis: 2001. Endocr Rev. 2001;22:53-74.

45 Rutter MM, Markoff E, Clayton L, Akeno N, Zhao G, Clemens TL, Chernausek SD. Osteoblast-specific expression of insulin-like growth factor-1 in bone of transgenic mice induces insulin-like growth factor binding protein-5. Bone. 2005;36:224-231.

46 Bautista CM, Baylink DJ, Mohan S. Isolation of a novel insulin-like growth factor (IGF) binding protein from human bone: a potential candidate for fixing IGF-II in human bone. Biochem Biophys Res Commun. 1991;176:756-763.

47 Jones JI, Gockerman A, Busby WH, Jr., Camacho-Hubner C, Clemmons DR. Extracellular matrix contains insulin-like growth factor binding protein-5: potentiation of the effects of IGF-I. J Cell Biol. 1993;121:679-687.

48 Waxman DJ, O'Connor C. Growth hormone regulation of sex-dependent liver gene expression. Mol Endocrinol. 2006;20: 2613-2629.

49 Ogita M, Rached MT, Dworakowski E, Bilezikian JP, Kousteni S. Differentiation and proliferation of periosteal osteoblast progenitors are differentially regulated by estrogens and intermittent parathyroid hormone administration. Endocrinology. 2008;149: 5713-5723.

50 Olson LE, Ohlsson C, Mohan S. The role of GH/IGF-I-mediated mechanisms in sex differences in cortical bone size in mice. Calcif Tissue Int. 20118;8:1-8.

51 Gennari L, Nuti R, Bilezikian JP. Aromatase activity and bone homeostasis in men. J Clin Endocrinol Metab. 2004;89:5898-907.

52 Liongue C, Ward AC. Evolution of Class I cytokine receptors. BMC Evol Biol. 2007;7:120.